

A Phantom and In Vivo Study of Mice Following an Ischemic Stroke Using Sodium MRI

Kun-Che Lee, Yi-Shin Lee, Guo-Jen Huang, Hsiao-Lung Chan, Jen-Fang Yu*

Abstract— Sodium is one of the essential indicators of cell viability in vivo. Regarding extant literature, sodium MRI is widely employed for various studies, including research on tumors, strokes, and neurocognition, because it can non-invasively provide data of physiological metabolism in vivo. Currently, strokes are among the 3 leading causes of death worldwide, and can be categorized as hemorrhagic or ischemic. Approximately 70% to 80% of stroke patients experience an ischemic stroke. Although numerous relevant studies have focused on larger animal models, such as rats, cats, and nonhuman primates, literature that employs mice experimental models is scarce. In this study, we conducted sodium MRI on the brains of mice after an ischemic stroke to observe sodium signal variations in the brain following this type of stroke. The findings indicated that the sodium signals in the brain regions affected by stroke were 2.3 times stronger than those in the lateral ventricles.

I. INTRODUCTION

Brain functions are supported by an adequate supply of oxygen and glucose through the normal circulation of blood. Therefore, changes in circulation can severely affect the brain and lead to a well-known cerebrovascular disease, that is, a stroke. Studies have reported that strokes are among the 3 leading causes of death worldwide, following cancer and cardiovascular disease [1]. Strokes are classified as either hemorrhagic or ischemic. Approximately 70% to 80% of stroke patients experience an ischemic stroke [2]. Therefore, this study focuses on investigating ischemic strokes.

Extant clinical studies have provided numerous imaging methods for diagnosing strokes, such as computer tomography(CT), diffusion MRI, and perfusion MRI. However, although these methods can rapidly and effectively identify the brain regions affected by a stroke, the viability of the brain cells in these regions cannot be determined; thus, additional imaging technologies are required [3]. Sodium and cell viability are closely related because abnormal sodium levels reduce cell viability. Therefore, magnetic

resonance(MR) technologies not only allow researchers to non-invasively observe the levels of certain ions in tissues, but also provide diagnosticians with additional physiological data, which can be integrated to provide an effective diagnosis.

Sodium is a key indicator of cell viability in vivo. According to extant literature, in contrast to proton MRI, which generates structural data, sodium MRI provides data regarding physiological metabolism in vivo [4]. Furthermore, sodium MRI can be used to evaluate physiological conditions. Thus, this technology is widely employed in various studies, including research on tumors, strokes, and neurocognition [5, 6]. However, despite the broad range of sodium MRI applications, sodium signals are weak, increasing the difficulty of image capturing. Consequently, the results of this technology are only employed in academic research and not used for clinical studies or diagnostics.

A number of extant studies related to ischemic strokes have reported on the use of sodium MRI, asserting that sodium concentrations increase in localized areas of the brain following an ischemic stroke. Previous literature has generally adopted larger animal models such as rats, cats, and nonhuman primates; the use of mice as experimental models is rare. This is because the brains of mice are comparatively smaller, which further increases the challenge of acquiring sodium signals.

Despite the difficulty of acquiring sodium signals from mice, this process is essential because it provides physiological data of mice brains, which can serve as a basis for future studies. This study employed sodium MRI technology to observe sodium signal variations in the brains of mice following an ischemic stroke.

II. MATERIALS AND METHODS

A. The phantom models

To effectively identify variations of the sodium concentrations in mice brains, 5 phantom samples of a sodium chloride (NaCl) solution at 40 mM, 70, mM, 100 mM, 140 mM, and 160 mM were verified before conducting in vivo mice experiments. Each solution sample was placed in a plastic tube with a diameter of 0.2 cm and length of 2.5 cm. The tube openings were then tightly sealed.

B. The animal models

For the experimental study, 6 male C57BL/6 mice approximately 6 weeks of age and weighing 20 g were obtained. The middle cerebral artery occlusion (MCAO) surgical procedure was performed on the mice to induce

Kun-Che Lee is with the Department of Electrical Engineering, Chang Gung University, Taoyuan, Taiwan, (e-mail: feather62j@hotmail.com).

Yi-Shin Lee is with the Department of Biomedical Sciences, Chang Gung University, Taoyuan, Taiwan, (e-mail: j3609333@hotmail.com).

Guo-Jen Huang is with the Department of Biomedical Sciences, Chang Gung University, Taoyuan, Taiwan, (e-mail: gjh30@mail.cgu.edu.tw).

Hsiao-Lung Chan is with the Department of Electrical Engineering, Chang Gung University, Taoyuan, Taiwan, (e-mail: chanhl@mail.cgu.edu.tw).

*Jen-Fang Yu is with the Graduate Institute of Medical Mechatronics, Chang Gung University, Taoyuan, Taiwan, (corresponding author, phone: 886-3-2118800 ext 5758, 5721; fax: 886-3-2118050; e-mail: jfyu.phd@gmail.com).

ischemia in localized areas of the right cerebral hemisphere. The middle cerebral artery was permanently occluded through cauterization before the right common carotid artery was temporarily occluded to exacerbate ischemia in the brain. The temporary occlusion was removed after 150 min. Finally, MRI was conducted 2 days after the surgery. The protocol was approved by the Institutional Animal Care and Use Committee of Chang Gung University.

C. Experimental setup

The experiments were conducted using a 7 Tesla small animal MRI instrument (BioSpec 70/30 USR, Bruker BioSpin GmbH, Germany) equipped with a double-tuned $^1\text{H}/^{23}\text{Na}$ surface coil to excite and receive signals. A surface coil with a 2 cm diameter was placed on the NMR imaging instrument. After the mice were heavily anesthetized using a mixture of 1% isoflurane and 100% pure oxygen, they were placed on the supporting platform and connected to external anesthetic machines to manage their anaesthetized state. The supporting platform was connected to a warm water circulation system to maintain the temperature of the mice during the experiment. Furthermore, the mice's respiratory conditions were monitored during the experiment to ensure their safety.

After completing the mice experiment setup, the sample side of the surface coil was fixed as close to the brain of the mice as possible for efficient signal acquisition. Subsequently, the supporting platform was moved to the center of the magnetic field before the coil parameters were set. The principal resonant frequency for hydrogen and sodium nuclides was 300.33 MHz and 79.44 MHz, respectively. After the hardware setup, ParaVision® 5.1 software was adopted to adjust the imaging parameters. The hydrogen principal resonant frequency was used for image positioning to confirm the placement of the mice brains. After positioning, hydrogen MRI scans were conducted.

D. Proton MR imaging of phantoms

Proton MRI scans were performed using a TurboRARE-T2 pulse sequence. The imaging parameters were as follows: TR = 2500 ms, TE = 33 ms, FOV = 2 cm \times 2 cm, matrix size = 128 \times 128, flip angle = 180°, NEX = 2, thickness = 2 mm, 1 slice, and scan time = 1 min 20 s.

E. Sodium MR imaging of phantoms

After conducting proton MR imaging, the nuclide frequency of the scanner was converted to the appropriate value for sodium imaging. The positioning slices of the proton MR images were used as the baseline, which facilitated sodium MRI scans of the positioning slices. The scans were conducted using a FLASH pulse sequence under the following parameters: TR = 90 ms, TE = 2.5 ms, FOV = 2 cm \times 2 cm, matrix size = 64 \times 64, flip angle = 30°, NEX = 50, thickness = 4 mm, 1 slice, and scan time = 4 min 48 s.

F. Proton MR imaging of in vivo mice

Proton MRI scans were performed using a TurboRARE-T2 pulse sequence. The imaging parameters were as follows: TR = 2500 ms, TE = 33 ms, FOV = 2.5 cm \times 2.5 cm, matrix size =

256 \times 256, flip angle = 180°, NEX = 4, thickness = 1.5 mm, 7 slices, and scan time = 5 min 20 s.

G. Sodium MR imaging of in vivo mice

After completing proton MR imaging, the nuclide frequency of the scanner was converted to the appropriate value for sodium imaging. The positioning slices of the proton MR image were used as the baseline. Three slice positions of the ischemic region were set as the slice images for the sodium MRI scan. Scanning was conducted using a FLASH pulse sequence and the following imaging parameters: TR = 90 ms, TE = 2.5 ms, FOV = 2.5 cm \times 2.5 cm, matrix size = 64 \times 64, flip angle = 30°, NEX = 300, thickness = 1.5 mm, 3 slices, and scan time = 28 min 48 s. The image resolution was 0.39 \times 0.39 mm².

H. Image analysis

The medical image analysis software Image J developed by the National Institutes of Health (USA) was used to analyze the MR images. The obtained images were imported into Image J, and the matrix size of the sodium images of the phantoms and mice brains were made equal to that of the proton images through interpolation. We identified and circled the regions of interest (ROIs) in the proton images of the 5 phantoms at various concentrations and the ischemia and contralateral areas of the mice brains. The corresponding position of these ROIs in the sodium images were identified and circled. Finally, the ROIs were measured for signal intensity.

III. RESULTS AND DISCUSSIONS

According to the properties of sodium nuclides, the rate of signal attenuation is typically faster; thus, a shorter echo time is required for signal acquisitions. Previous literature has reported that the gradient pulse sequence is the optimal imaging pulse sequence [7]. In addition, the FLASH sequence has been successfully applied in previous sodium MRI studies [8, 9]. Therefore, we used the FLASH sequence for the sodium images of the phantoms and mice. The implementation of this type of sequence is also comparatively easier.

Proton and sodium images of the phantoms are shown in Figs. 1a and 1b. The proton image (Fig. 1a) shows the relative positions of the 5 phantoms in the tubes with the following concentrations (in order from left to right): 40 mM, 70 mM, 100 mM, 140 mM, and 160 mM. The signal profiles of the proton image are shown in Fig. 2; the results indicate that the 5 phantoms exhibit evenly distributed signals. Regarding the sodium images, the contour of the phantom images sharpened with increases in the sodium concentration. The signal profiles of the sodium images are shown in Fig. 3. The results (Fig. 4) demonstrate that the sodium signal intensifies with increased concentrations. This phenomenon corresponds to the results observed in the sodium images. During correlation analysis, the sodium signal intensity of the 5 phantoms exhibited a significant correlation with sodium concentrations (R value = 0.984, P -value < 0.05).

Proton and sodium images of mice brains affected by an ischemic stroke are shown in Figs. 5a and 5b. To identify the areas where sodium signals appear, the images were processed using color encoding. Employing the lookup table (LUT), the original 256×256 grayscale images with values ranging between 0 and 255 were converted into corresponding color images. In cases of ischemic stroke, the ischemic areas of the brain were clearly apparent in the proton images. The signal intensity of ischemic areas was superior to that of contralateral areas. This phenomenon was also observed in the sodium images. Furthermore, the ischemic areas indicated were consistent in both the proton and sodium images. The average signal intensity for the 6 ROI groups of ischemia and contralateral areas is shown in Fig. 6. The results showed significant variation in the sodium signals between the left and right sides of the brain. Following a comparison, we found that the intensity of the sodium signal for ischemia areas was 2.3 times higher than that for contralateral areas. We also performed a paired samples *t*-test and confirmed that the sodium signals of the ischemia and contralateral areas differed significantly ($p < .05$). The average signal-to-noise (SNR) values for the 6 ROI groups of ischemia and contralateral areas are provided in Table 1.

The results of the phantom experiment confirmed that a positive correlation exists between the sodium signal intensity and sodium concentration. Generally, the difficulty of sodium detection is attributed to the low sodium concentration (45 mM) in brain tissues *in vivo* and the typically weak sodium signals. In previous studies, sodium was detected only in cerebrospinal fluids and tissue fluids at approximately 140 mM. After an ischemic stroke, because the sodium-potassium pumps in ischemia areas are affected, the cells cannot maintain homeostasis, preventing the ions in cells from being metabolized normally. Thus, sodium concentrations increase, enabling the detection of abnormal signals using sodium MRI.

Signal acquisition using sodium MRIs has always been a challenging process. However, the advancement of technologies and the development of hardware with greater magnetic fields and novel software for image acquisitions provide continuous opportunities for prospective researchers.

IV. CONCLUSION

In this study, we verified the feasibility of applying sodium MRI technology to mice brains. Using this technology, we observed variations in the sodium signal intensity of the phantoms at various concentrations. The technology was subsequently applied to mice to obtain ischemic stroke images. The findings of this study indicate that a significant correlation exists between sodium concentrations and sodium signal intensity. Moreover, the sodium signal intensity of ischemia areas was 2.3 times higher comparatively, which corresponds to the increase proposed in previous studies employing animal models. In the future, we intend to employ sodium images of mice brains to investigate sodium concentrations *in vivo* and also comparison with other different methods.

ACKNOWLEDGMENT

The authors thank the Functional Neuroscience Laboratory at Chang Gung University for its support with the animal surgeries, the 7T Animal MRI Core Laboratory of the Neurobiology and Cognitive Science Center for technical support and use of the facilities, and the Instrumentation Center at National Taiwan University for conducting the MRI experiments.

REFERENCES

- [1] S. G. Kanekar, T. Zacharia, and R. Roller, "Imaging of stroke: Part 2, Pathophysiology at the molecular and cellular levels and corresponding imaging changes," *AJR Am J Roentgenol*, vol. 198, pp. 63-74, Jan 2012.
- [2] J. B. Casals, N. C. Pieri, M. L. Feitosa, A. C. Ercolin, K. C. Roballo, R. S. Barreto, *et al.*, "The use of animal models for stroke research: a review," *Comp Med*, vol. 61, pp. 305-13, Aug 2011.
- [3] F. E. Boada, Y. Qian, E. Nemoto, T. Jovin, C. Jungreis, S. C. Jones, *et al.*, "Sodium MRI and the Assessment of Irreversible Tissue Damage During Hyper-Acute Stroke," *Transl. Stroke Res.*, vol. 3, pp. 235-45, 2012.
- [4] R. Ouwerkerk, "Sodium magnetic resonance imaging: from research to clinical use," *J Am Coll Radiol*, vol. 4, pp. 739-41, Oct 2007.
- [5] R. Ouwerkerk, "Sodium MRI," *Methods Mol Biol*, vol. 711, pp. 175-201, 2011.
- [6] Y. Qian, T. Zhao, H. Zheng, J. Weimer, and F. E. Boada, "High-resolution sodium imaging of human brain at 7 T," *Magn Reson Med*, vol. 68, pp. 227-33, Jul 2012.
- [7] T. B. Parrish, D. S. Fieno, S. W. Fitzgerald, and R. M. Judd, "Theoretical basis for sodium and potassium MRI of the human heart at 1.5 T," *Magn Reson Med*, vol. 38, pp. 653-61, Oct 1997.
- [8] F. Wetterling, M. Hogler, U. Molkenthin, S. Junge, L. Gallagher, I. Mhairi Macrae, *et al.*, "The design of a double-tuned two-port surface resonator and its application to *in vivo* hydrogen- and sodium-MRI," *J Magn Reson*, vol. 217, pp. 10-8, Apr 2012.
- [9] M. Augath, P. Heiler, S. Kirsch, and L. R. Schad, "In vivo(39)K, (23)Na and (1)H MR imaging using a triple resonant RF coil setup," *J Magn Reson*, vol. 200, pp. 134-6, Sep 2009.

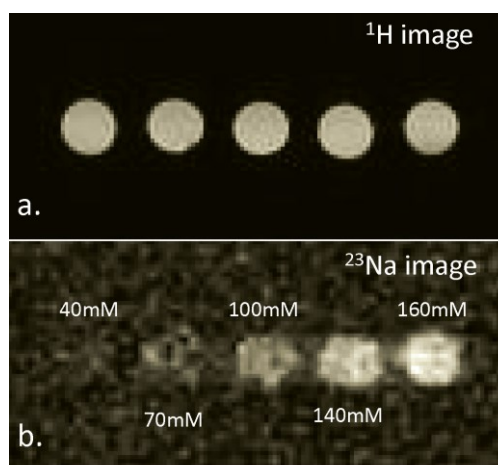


Figure 1. Images of phantoms in 5 NaCl solution concentrations: (a) proton image, (b) sodium image

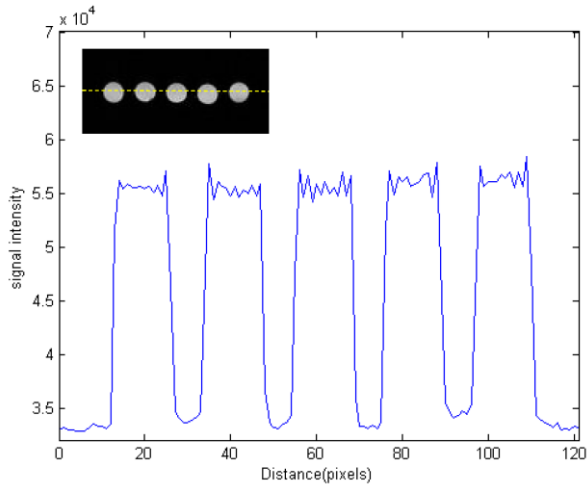


Figure 2. Signal profile of the proton images

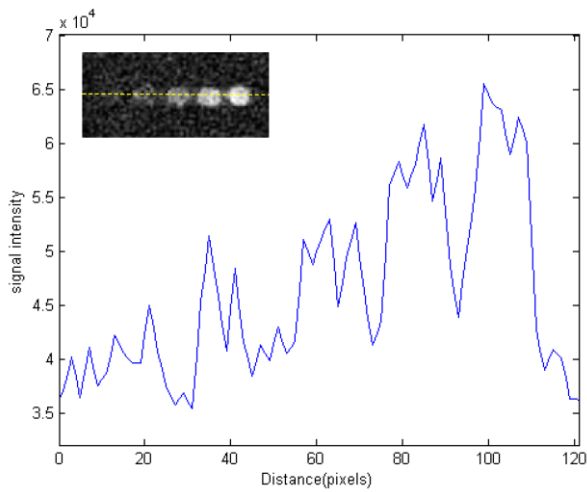


Figure 3. Signal profile of the sodium images

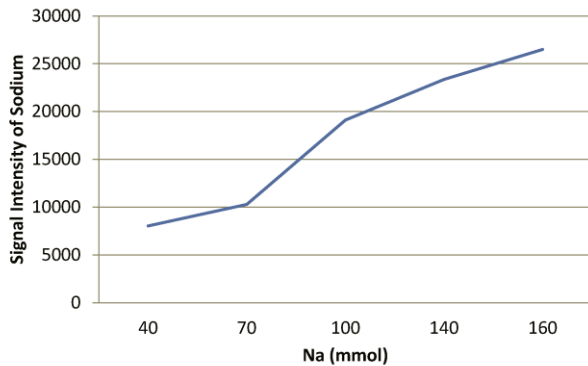


Figure 4. The relationship between the image signal intensity and sodium concentrations

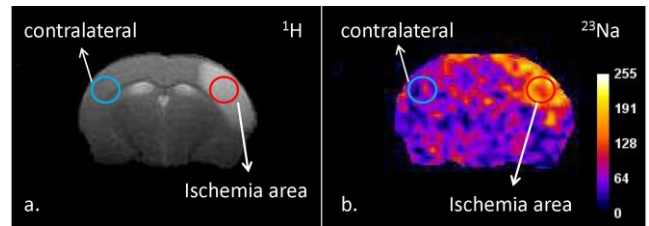


Figure 5. Images of mice brains affected by ischemic stroke: (a) proton image, and (b) sodium image

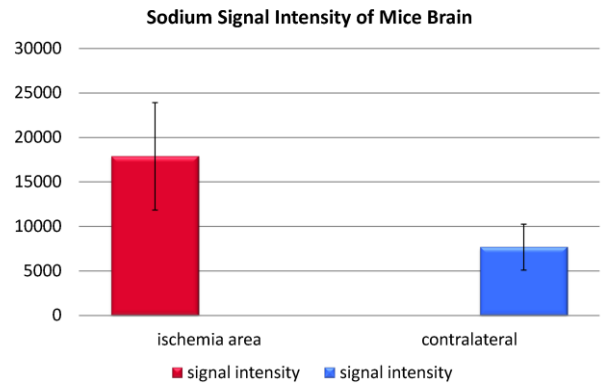


Figure 6. The average signal intensity of mice brains

Table 1. SNR value of the ischemia and contralateral areas

	SNR of sodium imaging
ROIs in the ischemic area	10.3
ROIs in the contralateral area	4.7